Research Article

Eliana Nope, Ángel G. Sathicq, José J. Martínez, Zeid A. ALOthman, Gustavo P. Romanelli, Elena Montejano Nares, Francisco Ivars-Barceló, Juan Rubio Zuazo, Rafael Luque*, and Alina M. Balu*

Revisiting hydrotalcite synthesis: Efficient combined mechanochemical/coprecipitation synthesis to design advanced tunable basic catalysts

https://doi.org/10.1515/ntrev-2024-0042
received December 11, 2023; accepted May 17, 2024

Abstract: Hydrotalcite materials (HTs) were synthesized by a facile and swift combined mechanochemistry/coprecipitation approach, and their catalytic activity was evaluated and compared with conventionally synthesized hydrotalcites (co-precipitation method) in the Knoevenagel condensation between furfural and ethyl cyanoacetate/malononitrile. Characterization and catalytic activity results clearly demonstrate that the proposed combined mechanochemical/coprecipitation approach provides an improvement in crystallinity, morphology, tunable basicity, and textural properties (higher surface area and enhanced surface properties) as compared to HTs obtained *via* conventional coprecipitation methods. In addition, mechanochemically synthesized HTs largely improve catalytic activities, including conversion and product selectivity to Knoevenagel condensation products under solventless conditions, short reaction times, or reaction at room temperature as compared to conventional counterparts (*e.g.*, 30–40 *vs* > 99% product yields).

*** Corresponding author: Rafael Luque**, Peoples Friendship University of Russia (RUDN University), 6 Miklukho Maklaya str., 117198, Moscow, Russian Federation; Universidad ECOTEC, Km. 13.5 Samborondón, Samborondón, EC092302, Ecuador, e-mail: rluque@ecotec.edu.ec
*** Corresponding author: Alina M. Balu**, Department of Organic Chemistry, University of Cordoba, Rabanales Campus, Marie Curie Building (C-3), Ctra Nnal IV-A, Km 396, E14014, Córdoba, Spain, e-mail: qo2balua@uco.es
Eliana Nope: Department of Organic Chemistry, University of Cordoba, Rabanales Campus, Marie Curie Building (C-3), Ctra Nnal IV-A, Km 396, E14014, Córdoba, Spain; Center for Research and Development in Applied Sciences "Dr. Jorge J. Ronco" CINDECA, Faculty of Exact Sciences, National University of La Plata, 47 N_ 257, La Plata, 1900, Argentina
Ángel G. Sathicq: Center for Research and Development in Applied Sciences "Dr. Jorge J. Ronco" CINDECA, Faculty of Exact Sciences, National University of La Plata, 47 N_ 257, La Plata, 1900, Argentina
José J. Martínez: School of Chemical Sciences, Faculty of Sciences, Pedagogical and Technological University of Colombia UPTC, Avenida Central del Norte, Tunja, Boyacá, 150003, Colombia
Zeid A. ALOthman: Chemistry Department, College of Science, King Saud University, P.O. Box 2455, Riyadh, 11451, Saudi Arabia
Gustavo P. Romanelli: Center for Research and Development in Applied Sciences "Dr. Jorge J. Ronco" CINDECA, Faculty of Exact Sciences, National University of La Plata, 47 N_ 257, La Plata, 1900, Argentina; CISAV, Department of Organic Chemistry, Faculty of Agricultural and Forestry Sciences, National University of La Plata, La Plata, Argentina; Forestry, National University of La Plata, Calles 60 y 119 s/n, La Plata, B1904AAN, Argentina
Elena Montejano Nares: Department of Organic Chemistry, University of Cordoba, Rabanales Campus, Marie Curie Building (C-3), Ctra Nnal IV-A, Km 396, E14014, Córdoba, Spain; Department of Inorganic Chemistry and Technical Chemistry, Faculty of Sciences, UNED; Av. España s/n, Las Rozas, 28232, Madrid, Spain
Francisco Ivars-Barceló: Departamento de Química Inorgánica y Química Técnica, Facultad de Ciencias, UNED; Av. España s/n, Las Rozas, 28232, Madrid, Spain
Juan Rubio Zuazo: SpLine CRG BM25 Beamline, The European Synchrotron, 71, Avenue des Martys, 38000, Grenoble, France; Instituto de Ciencia de Materiales de Madrid, Consejo Superior de Investigaciones Científicas (ICMM-CSIC), 28049, Madrid, Spain

1 Introduction

Layered double hydroxides (LDH), known as hydrotalcite (HT), are basic materials with a layered structure, which present divalent and trivalent cations and belong to the family of anionic clays. Generally, the structure of these materials is described starting from $Mg(OH)_2$ layers with a brucite-type structure, where Mg^{2+} cation coordinates six times with hydroxyl groups, forming octahedrons that share their edges with neighboring atoms, creating two-dimensional

sheets. These sheets are stacked on top of the other, forming layered networks held together by hydrogen bonds. The substitution of a fraction of the divalent cations in the brucite layer by trivalent cations generates a layer with a positive charge, which is compensated by anions in the interlamellar space, where crystallization water is also found [1,2]. The wide spectrum of divalent and trivalent cations, as well as interlamellar anions, have allowed the design of a wide variety of hydrotalcite with specific properties for various catalytic processes, becoming increasingly important in chemical synthesis [3].

HTs can be synthesized using various methodologies, such as hydrothermal treatment, coprecipitation, and sol–gel method, among others, with coprecipitation being the most widely utilized method in the literature. However, this methodology requires prolonged synthesis times (4 or more days), which makes the process highly time and energy-consuming [4,5]. Several investigations have focused on finding viable routes that allow a reduction in synthesis times for the preparation of these materials, with mechanochemistry proven to be a promising green alternative for such syntheses due to its versatility and simplicity [6,7].

Chitrakar *et al.* [8] described a solvent-free procedure for the synthesis of Zn Al-LDH, first grinding and then autoclaving the solid precursors at 150°C for 24 h. Tongamp *et al.* synthesized meixnerite, a type of layered hydroxide, grinding anhydrous magnesium and aluminum hydroxides in a planetary ball mill for 1 h and later for 2 h in the presence of water [9]; this was milled again with a certain amount of magnesium nitrate in the second stage for another 2 h [10]. Salmones *et al.* used the grinding process for 44 h on hydrotalcites synthesized by the coprecipitation method [11]. Mg-Al-LDHs were synthesized by manual grinding for 1 h in the absence of water; however, the results showed low crystallinity, so they were peptized to improve their properties [12]. CaAl-layered double hydroxide was obtained from two grinding stages: the first consisting of dry grinding of the precursors for 1 h, followed by the addition of water and grinding for 2 h [13]. Li-Al-OH LDH was synthesized by combining the grinding process and hydrothermal treatment. For this, the aluminum precursor $Al(OH)_3$ was first ground for 1 h, followed by the addition of the $LiOH{\cdot}H_2O$ precursor and ground for an additional 1 h; finally, it was subjected to hydrothermal treatment at 80°C for 1 h [14]. Madhusha *et al.* synthesized ascorbic acid intercalated layered double hydroxides (AA-LDHs) by milling NaOH pellets with magnesium and aluminum nitrates (the molar ratio of Mg and Al was 2:1) using manual milling for 1 h. The resulting solid was washed with distilled water and dried, mixed with ascorbic acid and NaOH, and manually milled for 1.5 h [15]. For the synthesis of Cu–Al layered double hydroxide and a methyl orange (MO)-intercalated one (MO-LDH), copper and aluminum precursors were ground for 2 h and then stirred in water or methyl orange solution for 4 h [16]. Chlorine-intercalated Mg–Al layered double hydroxides (Mg–Al–Cl–LDH) were synthesized using a one-step mechanochemistry method with high purity after 5 h of milling. Fahami *et al.* studied different grinding times and found that 1 h of grinding is not enough to form the hydrotalcite-type structure and that grinding times longer than 5 h significantly affect the structure of these materials [17]. In another investigation, these authors compared the hydrothermal method with the mechanochemical method for hydrotalcite synthesis and found that the characteristic layered structure for these materials can be simple and swiftly obtained using a ball mill as compared to that synthesized by the hydrothermal method. However, better crystallization was still achieved using the hydrothermal method [18].

Recently, $Mg_2Al\text{-}CO_3$ LDHs were synthesized by grinding a mixture of magnesium and aluminum hydroxide in a planetary ball milling for 5 h. Water was added to the resulting solid and was stirred for 30 h at 95°C [19]. Although these processes present a reduction in the synthesis time compared to the conventional coprecipitation method, all require high-energy consumption and yield materials with low crystallinity, according to literature reports.

This work presents a new methodology that combines the mechanochemical process (using a ball mill) with coprecipitation for the synthesis of advanced hydrotalcite systems, significantly shortening the synthesis time, improving crystallinity, and with the possibility of controlling basicity, all remarkably beneficial to enhance their catalytic activity. HTs were synthesized using different grinding times (10, 30, and 60 min), and their catalytic activity was tested in the Knoevenagel condensation reaction under solvent-free conditions with respect to conventionally synthesized HTs, offering significantly improved tunability and catalytic activity.

2 Experimental

2.1 Synthesis of hydrotalcites using the coprecipitation method

Layered double hydroxides with the general formula $M^{2+}_{1-x}M^{3+}_x(OH)_2CO_3{\cdot}nH_2O$ were synthesized using the coprecipitation method detailed in our previous work [20]. A M^{2+}/M^{3+} ratio of 3 with x = 0.25 was employed. Initially, 2.56 g of $Mg(NO_3)_2{\cdot}6H_2O$ and 1.35 g of $Al(NO_3)_3{\cdot}9H_2O$ were dissolved in 10 mL of distilled water in a 250 mL flask, and the solution was stirred for 20 min. Then, 2.91 g of urea was added to the

solution, followed by continuous stirring for 12 h at 60°C. Subsequently, the temperature was increased to 100°C, and stirred for an additional 24 h. Finally, a 2 M alkaline solution containing NaOH and Na_2CO_3 was gradually added until the pH reached 10. The resulting mixture was allowed to age for 24 h at 140°C. The white precipitate obtained was filtered, washed with distilled water, and dried overnight at 80°C. The resulting solid is denoted as HT-C.

The molar ratio [urea]/[NO_3] greater than 1 leads to the formation of NH_3 and CO_2, as the pH during the hydrolysis process remains close to 9 (HTs were synthesized at a molar ratio [urea]/[NO_3] = 3). Therefore, the carbonate provided by the decomposition of urea serves as the compensating anion in the HT phase, which follows the following reaction mechanism [21,22]:

$$NH_2{-}CO{-}NH_2 + 3H_2O \rightarrow NH_4^+ + CO_3^{2-}$$

$$(NH_4)_2CO_3 \rightarrow 2NH_3 \uparrow + CO_2 \uparrow + H_2O$$

$$NH_3 + H_2O \leftrightarrow NH_4OH \leftrightarrow NH_4^+ + OH^-$$

$$CO_2 + H_2O \leftrightarrow H_2CO_3 \leftrightarrow H^+ + HCO_3^- \leftrightarrow 2H^+ + CO_3^{2-}$$

$$OH^- + (1-x)Mg^{2+} + xAl^{3+} + (x/2)CO_3^{2-} + yH_2O \rightarrow [Mg(1-x)Alx(OH)_2](CO_3)x/2 \cdot yH_2O$$

$$18OH^- + 6Mg^{2+} + 2Al^{3+} + 9CO(NH_2)_2 + 12H_2O \rightarrow Mg_6Al_2(OH)_{16}CO_3 \cdot 4H_2O + 18NH_3 + 8CO_2$$

A 2M alkaline solution with a molar ratio of 1:1 (NaOH and Na_2CO_3) was prepared by dissolving NaOH in distilled water. Then, Na_2CO_3 and distilled water were slowly added until the desired final volume was reached (creating an entirely alkaline solution). The mixture was then continuously stirred until a translucent solution was obtained.

2.2 Synthesis of hydrotalcites by the combined mechanochemistry/coprecipitation method

Layered double hydroxides with the general formula $M^{2+}_{1-x}M^{3+}_x(OH)_2CO_3{\cdot}nH_2O$ were synthesized using a combination of mechanochemistry and the coprecipitation method. The mechanochemical step was conducted in a planetary ball mill (PM 100 from Retsch, 50 mL stainless steel vessel, and stainless steel 18 balls of 10 mm diameter). The synthesis was carried out using a M^{2+}/M^{3+} ratio = 3 and consisted of two stages. Initially, the precursor salts of divalent and trivalent cations were mixed with urea, employing the same amounts described above for the coprecipitation method, but this time utilizing a mechanochemical method, *i.e.*, ball milling at 300 rpm for 5 min. Subsequently, the resulting mixture was dissolved in distilled water (50 mL), and the pH was adjusted to 10 by slowly adding a 2 M alkaline solution of NaOH and Na_2CO_3. The solid obtained by coprecipitation was returned to the grinding process for 5 min at 300 rpm (second stage). Finally, the resulting solid was washed several times with distilled water and dried at 80°C for 12 h (Scheme 1). This process was also conducted using different syntheses times, aiming to complete 30 and 60 min of the milling process. In this regard, the first stage comprised mixing the precursor salts with an M^{2+}/M^{3+} ratio of 3 and urea, followed by grinding

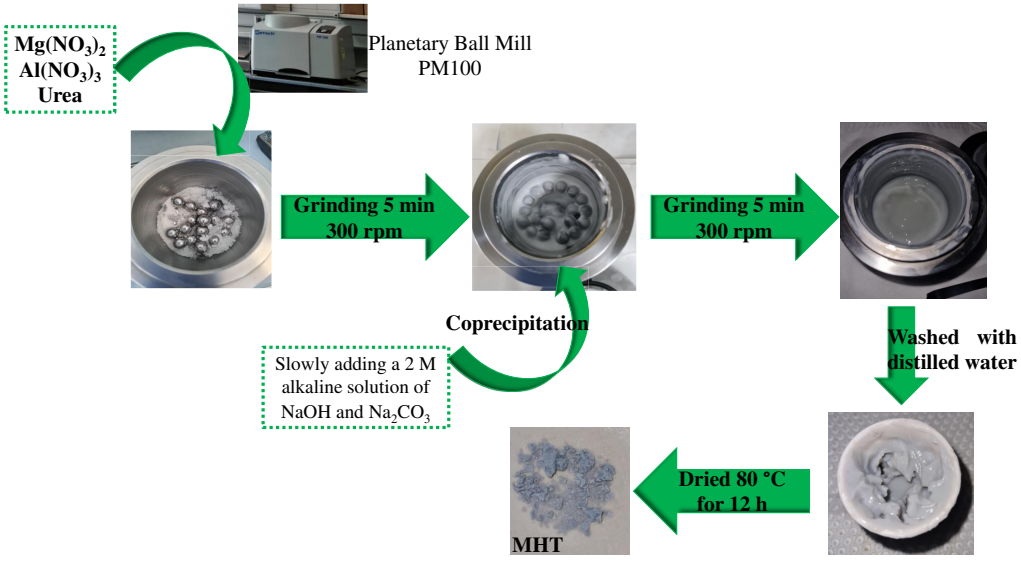

Scheme 1: Synthesis of hydrotalcites by the combined mechanochemistry/coprecipitation method.

(15 and 30 min). Once the pH reached 10, adjusted with a 2 M alkaline solution of NaOH and Na_2CO_3, the solid obtained by coprecipitation was returned to the grinding process for 15 and 30 min, respectively. The resulting solids are henceforth denoted as MHT10, MHT30, and MHT60.

2.3 Characterization of the hydrotalcite materials

Conventional X-ray diffraction (XRD) analysis of powder samples was performed using a Bruker D8 Discover diffractometer (Bruker, German) operated at a voltage of 40 kV and a current of 40 mA, with Cu $k\alpha$ (k = 1.54056 Å) radiation in the 2Θ range of 5°–80°, a count time of 1 s, and a step size of 0.05° s^{-1}. Further crystallography analyses were carried out using high-resolution X-ray diffraction (HR-XDR) with synchrotron light source radiation. These experiments were performed in the BM25-SpLine beamline at the European Synchrotron Radiation Facility (ESRF) in Grenoble (France) [23]. HR-XRD diffractograms were collected employing a step size of 0.02° s^{-1} with an incident wavelength of 0.8 Å and an excitation energy of 15.5 keV.

Textural properties were measured by N_2 isotherms at 77 K using a Micromeritics ASAP 2000 porosimeter. The samples were previously degassed at 100°C for 12 h. The surface area was calculated using a Brunauer–Emmett–Teller (BET) multipoint model. Infrared spectra (IR) were obtained with a Nicolet iS50 spectrometer by the ATR method, using sample dilution in KBr at a concentration of approximately 10%. SEM-FEI Quanta200 scanning electron microscope (SEM) was used to observe the surface structure of the samples and the shape of particles. IR spectra were obtained at a resolution of 4 cm^{-1} in the middle IR (4,000–400 cm^{-1}). CO_2 adsorption was measured using a Thermo Scientific model Nicolet iS50 FT-IR spectrometer, and infrared spectra were collected by the DRIFTS method. The materials were cleaned with a He flow of 30 mL/min at 100°C for 30 min. After the He flow, the adsorption of CO_2 was carried out at room temperature. In addition, volumetric titration with benzoic acid was carried out to measure the proportion of basic sites. In this method, 0.025 g of catalyst, a 0.01 M benzoic acid solution, and 1 mL of phenolphthalein (strong basic sites indicator) and bromothymol blue (weak basic sites indicator) were used.

2.4 Catalytic studies

The Knoevenagel condensation reaction between furfural and ethyl cyanoacetate was selected as a model reaction to evaluate the activity of the synthesized materials under solvent-free conditions (Scheme 2). Furfural (1 mmol), ethyl cyanoacetate or malononitrile (1 mmol), and 80 mg of catalyst were mixed in a reaction vessel and heated at 25, 40, and 80°C, respectively, for 10 or 30 min under magnetic stirring. After the reaction, acetone was added as an extraction solvent. Finally, the catalyst was separated and washed with acetone (3 × 2 mL), and dried at 80°C to evaluate its reusability. Quantitative analysis was conducted by gas chromatography using a series II Agilent 5890 GC, equipped with a Supelco Equitytm-1 (60 m × 0.25 mm × 0.25 µm) column and an FID detector (Supelco Analytical, Bellefonte, PA, USA). The temperature in the injector was 280°C. The oven temperature program used was as follows: initial temperature of 70°C for 1 min, ramped up to 190°C at a heating rate of 3°C/min, and remained constant at that temperature for 6 min. The products were identified using GC-MS.

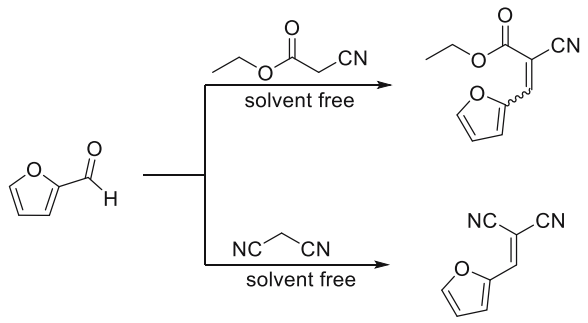

Scheme 2: Knoevenagel condensation of furfural with ethyl cyanoacetate/malononitrile.

3 Results and discussion

The crystalline properties of the synthesized materials were studied using powder X-ray diffraction. Generally, the coprecipitation method leads to the formation of a layered structure with high crystallinity; however, after long synthesis times (ca. 48 h). In this work, the synthesis of hydrotalcites was carried out by combining mechanochemistry using ball milling followed by the coprecipitation method in short synthesis times (typically 10 min).

X-ray diffraction patterns for these materials (10-, 30- or 60-min milling) are shown in Figure 1. In all cases, the strongest diffraction appears at 2Θ 11.3°, followed by that at 22.8° and three weaker lines at ca. 34.3°, 60.1°, and 61.6°, as well as two characteristic broad bands with the maximum centered at 38.4° and 45.5°. These line maxima and their relative intensities match those from JCPDS ref 22-0700, being fully consistent with those reported for carbonate-

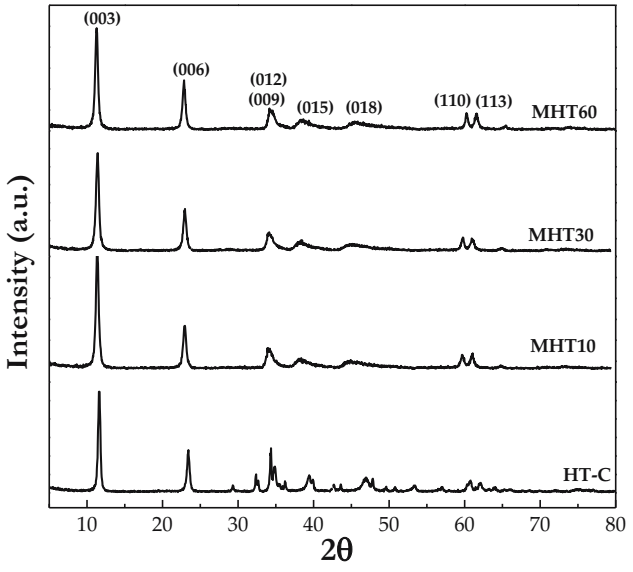

Figure 1: XRD patterns of HTs synthesized by the conventional coprecipitation method (HT-C sample) *vs* the novel combined mechanochemistry/coprecipitation strategy (MHT10, MHT30, and MHT60 samples).

intercalated Mg–Al layered double hydroxide with Mg:Al ratio of 3 [24], which is also in good agreement with the nominal Mg:Al ratio employed in the syntheses. This phase was described as a disordered structure containing a random sequence of rhombohedral and hexagonal stacking layers or $3R_1$ and $2H_1$ polytypes [24].

The formation of layered structures is confirmed by the presence of diffractions at 11.3°, 22.8°, and 34.3°, which correspond to the (003), (006), and (009) planes, respectively, and indicate multilayer stacking [25]. From the maximum of the reflection associated with the (003) plane, the interplanar distance or basal spacing *d* of the HT structure can be calculated (*e.g.*, 7.78 Å for MHT10). The spacing *d* between consecutive layers corresponds to the *c* parameter of the unit cell, *i.e.,* 23.35 Å for MHT10 [26]. The reflection related to the (110) plane is not dependent on the layer stacking arrangement [24], which is used to calculate the parameter *a* (equal to parameter *b*) as twice $d_{(110)}$, *i.e.*, 3.08 Å for MHT10.

Most importantly, powder XRD patterns of the solid obtained using the conventional coprecipitation method (employing ca. 48 h of synthesis) exhibit a higher number of narrow diffractions, with the absence of the broad bands displayed for HTs obtained by the combined mechanochemical/coprecipitation approach. In general, the pattern shows a significantly more complex X-ray diffractogram with a larger number of overlapped lines, which point to a mixture of phases.

Aiming to identify different crystalline phases, high-resolution X-ray diffraction (HR-GIXRD) experiments using synchrotron light source radiation were subsequently performed for both conventionally synthesized (HT-C) *vs* combined mechanochemical/coprecipitation method (MHT10), as depicted in Figure 2. The high-resolution diffractogram confirmed the complete absence of impurities in MHT10 prepared by the novel combined method as compared to several mixed phases clearly observed for HT-C, even after 48 h coprecipitation synthesis. The 2θ maximum positions and relative intensities, characteristic of a hydrotalcite with rhombohedral R3m structure and chemical formula $Mg_6Al_2(CO_3)(OH)_{16}{\cdot}4H_2O$, reported as JCPDS ref. 00-041-1428 [27], was found in the HR-XRD pattern of HT-C. The reflections of this hydrotalcite phase are displayed together with those characteristic of a mixed carbonate phase, denoted as Eitelite (JCPDS ref. 00-025-0847), described as a rhombohedral R3 structure with chemical formula $Na_2Mg(CO_3)_2$ [28]. Additionally, MgO (JCPDS ref. 00-043-1022) and Na_2O (JCPDS ref. 00-003-1074) appeared as minor crystalline phases.

The formation of the observed phases in HT-C obtained by the coprecipitation method may arise from several mechanisms, including partial hydroxylation occurring during the initial synthesis stage, where MgO transforms to $Mg(OH)_2$, or the formation of highly stable intermediates, such as $MgCO_3$ and $Al(OH)_3$, which potentially engage in reactions with the alkaline solution composed of NaOH and Na_2CO_3 [29,30]. While the hydrolysis of urea generates carbonate ions (CO_3^{2-}), the combined approach of coprecipitation and urea hydrolysis

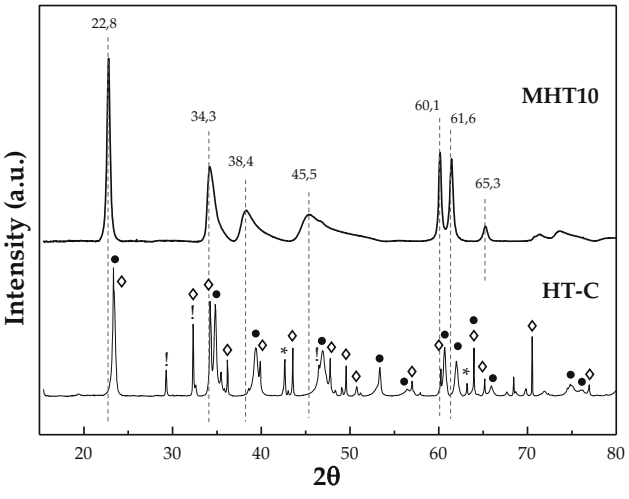

Figure 2: High-resolution powder XRD patterns of the solid prepared by the conventional co-precipitation method (HT-C), and the most representative solid obtained by combining the mechanochemistry method and coprecipitation using 10 min of synthesis time (MHT10). Symbols: $Mg_6Al_2(CO_3)(OH)_{16}{\cdot}4H_2O$ phase with JCPDS ref. 22-0700 (numbers above the dotted lines), $Mg_6Al_2(CO_3)(OH)_{16}{\cdot}4H_2O$ phase with JCPDS ref. 00-041-1428 (•), $Na_2Mg(CO_3)_2$ Eitelite phase with JCPDS ref. 00-025-0847 (◊), MgO phase with JCPDS ref. 00-043-1022 (*), and Na_2O phase with JCPDS ref. 00-003-1074 (!).

may serve to finely modulate the nucleation and crystallization processes, thereby fostering the development of hydrotalcite structures characterized by their fine and homogeneous morphology [22,31]. Nevertheless, the emergence of alternative phases *via* the coprecipitation method could also be contingent upon factors such as the concentration of metal precursors, the quantity of urea utilized, the alkaline solution concentrations, temperature, the pH value needed for the precipitation, and aging time [30,32]. Consequently, the synergistic employment of mechanochemical and coprecipitation methodologies represents a compelling strategy for achieving hydrotalcites with high purity in a short time.

The unit cell parameters calculated for the hydrotalcite phase contained in HT-C were a = 3.05 Å and c = 22.84 Å. These parameters are significantly lower than those found for MHT10 (a = 3.08 Å and c = 23.35 Å). Remarkably, MHT10 exhibits a more expanded structure than HT-C, either within layers or between them. Considering that parameter a corresponds to the closest average cation–cation distance within a layer [33,34], and a higher a indicates an increase in Mg content with respect to Al, as the ionic radius of Mg^{2+} (0.065 nm) is comparatively larger than that of Al^{3+} (0.050 nm) [35,36]. These facts are in good agreement with the accompanying increase obtained in the interlayer distance, related to the observed increase in parameter c. The enhancement of interlayer distance is generally related to the lower number of carbonate anions, which are partially substituted with bicarbonates (HCO_3^-) due to a decrease in the cationic charge from the brucite layer to be compensated [37,38]. In essence, these results clearly pointed out that the proposed combined mechanochemical/coprecipitation approach offers access to highly pure and crystalline LDHs in short times (10 min), with no significant differences observed among powder XRD patterns for MHT materials regardless of the synthesis time (10–60 min milling).

The average crystallite size values, determined by the Scherrer equation, are listed in Table 1. It is evident that the milling time influences the crystallite size, with longer milling times (1 h) resulting in larger crystallite sizes, while shorter times result in smaller sizes. In the case of HT-C, a larger crystallite size is obtained compared to the rest of the synthesized materials. These outcomes can be linked to the nucleation and crystallization processes occurring during the synthesis. Nucleation initiates upon adding an alkaline solution at constant pH to a solution containing precursor metal salts of M^{2+} and M^{3+} cations, and simultaneously, crystal growth begins with the addition. Several authors have reported that these processes affect crystallinity and crystallite size, being highly influenced by temperature and time in the synthesis. Coral *et al*. studied different microwave irradiation times in the synthesis of HT and observed that with 300 min of irradiation at 110°C, crystalline properties significantly improved compared to 10 min of microwave irradiation at the same temperature [39]. In treatments involving hydrothermal conditions at increasing temperatures and longer aging times, crystallinity and crystallite size tend to increase [40,41].

The results obtained from the combination of mechanochemistry/coprecipitation suggest that the change in the crystallite size depends on the second milling stage after coprecipitation, where nucleation and crystal growth processes occur simultaneously and are influenced by milling time; longer milling time in this stage generates larger crystallite sizes. In the first stage, milling of the metal precursors with urea allows them to be reduced to an amorphous phase, creating active sites for water molecules and compensation anions to be incorporated into the structure [10]. However, for HT-C, these processes occur during coprecipitation and aging, which require more synthesis time, resulting in a larger crystallite size.

The slight change in the crystallite size (approximately 1.5 nm) in the synthesis methods for HTC and MHT suggests that these results could primarily be related to the presence of urea, which finely modulates nucleation and crystallization processes, as described above. The small crystallite sizes observed for MHT materials may indicate high particle agglomeration. Since the crystallite size in D_{003} is related to the stacking distance of layers like brucite [42], it is plausible that the structure widens due to the agglomeration of extremely small particles, as evidenced by the "c" parameter value for MHT10. The presence of small crystallites suggests a higher amount of grain boundaries and surface defects, which could increase the surface reactivity of the materials as well as lead to a greater number of pores or the formation of small pores.

Textural properties of the synthesized HTs are summarized in Table 1. All pure solids (carbonate-intercalated Mg–Al layers double hydroxide) synthesized by the novel combined mechanochemical method also exhibited remarkably improved surface areas (ca. 70–80 $m^2 g^{-1}$)

Table 1: Textural properties of hydrotalcites synthesized and crystallite sizes

Catalyst	S_{BET} ($m^2 g^{-1}$)	Pore volume ($cm^3 g^{-1}$)	Pore size (nm)	Crystallite size* (nm)
HT-C	17	0.11	8	4.1
MHT10	88	0.29	13	2.7
MHT30	78	0.39	20	2.7
MHT60	63	0.31	18	3.5

*$D_{(003)}$ was calculated using the Scherrer equation.

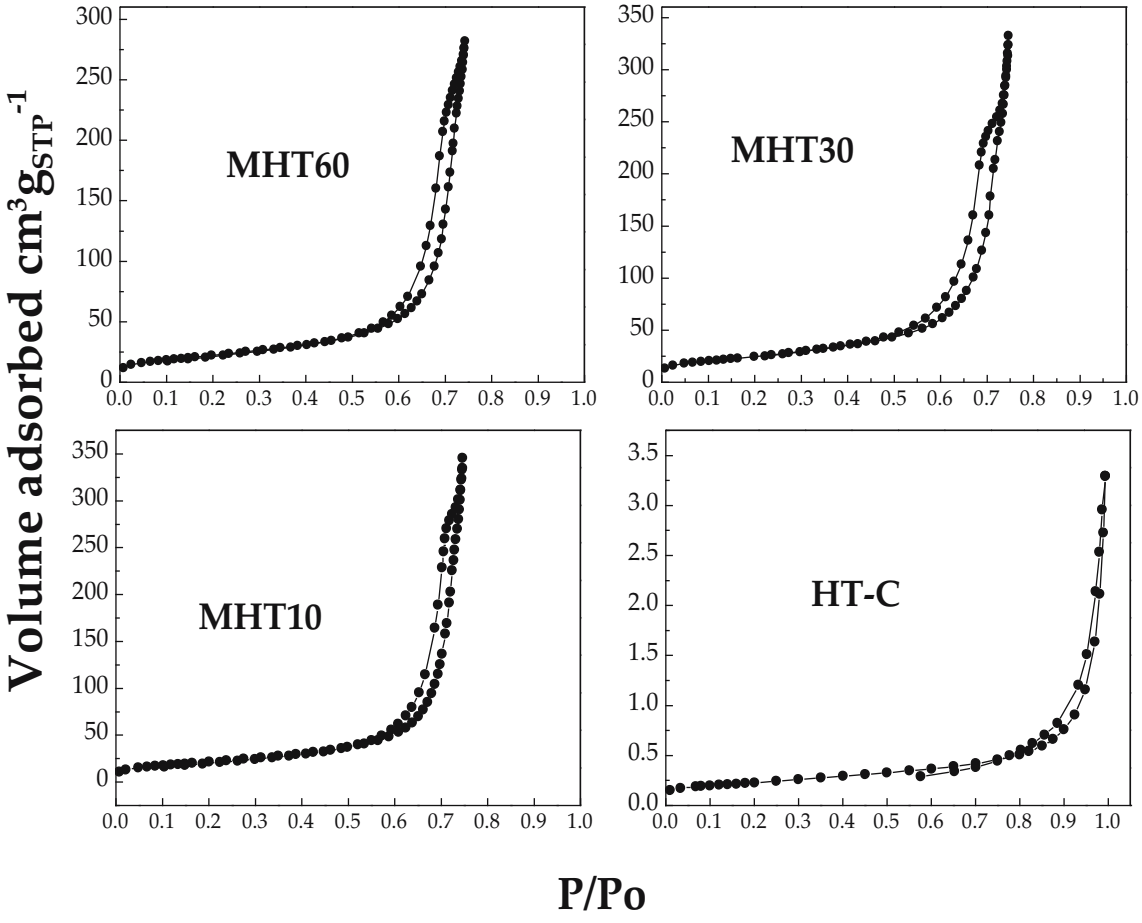

Figure 3: N_2 adsorption–desorption isotherms of hydrotalcites synthesized by the combined mechanochemical/coprecipitation method (MHT10, MHT30, MHT60) as compared to conventional coprecipitation method (HT-C, shown in the inset due to the difference in adsorbed volumes).

compared to conventionally synthesized HTs, which are typically poorly porous-defined (usually <20 $m^2 g^{-1}$). Volume and, importantly, pore size (potentially relevant for catalysis and adsorption applications) also significantly improved for materials synthesized *via* the combined mechanochemically/coprecipitated method, likely due to the alteration in microscopic morphology related to the presence of different cations within the layered structure (isomorphic substitution of divalent cations [43]), which are highly favored under mechanochemical conditions. The intimate mixing (and enhanced interaction) between the precursor salts of the divalent and trivalent cations during ball milling leads to the formation of bicarbonate species, significantly enhancing the textural properties of the combined mechanochemical/coprecipitation materials, as described in the XRD analysis. Therefore, this synthesis method enables achieving results comparable to those obtained with hydrotalcites synthesized by other methods [44–47]; however, this work highlights short synthesis times.

The grinding time significantly influences the textural properties of the materials, as observed in the comparison in Table 1, where the surface area decreases with grinding time, indicating that a grinding time of 10 min could represent an optimal time. However, the volume and pore size values do not follow this trend. The change in the textural properties of MHT is linked to particle growth. Previous research, such as that by Benito *et al.*, explored the synthesis of hydrotalcites using different microwave irradiation times and found that an increase in irradiation time leads to a decrease in surface area, associating these results with hydrotalcite particle growth [48]. In our synthesis process, changes in textural properties could also be attributed to particle agglomeration and modification over the grinding time. This suggests that, despite presenting similar surface areas, pore size and distribution vary within these materials, as described later. This phenomenon arises because the porosity of layered double hydroxides emerges due to the imperfect fitting of particles in a hexagonal sheet form, which can result in slit-shaped pore formation [49].

Adsorption–desorption isotherms of the synthesized materials are shown in Figure 3, with all solids exhibiting type IV isotherms, characteristic of mesoporous materials with hysteresis loop H3 [50]. This type of loop indicates the formation of materials in the form of plates, where particle pores have slit shapes, characteristic of hydrotalcite-type materials [51]. Although the shape of the isotherms is the same in all cases, the adsorption capacity (approximately taken from the amount of nitrogen adsorbed at a relative pressure of 0.95) in HT-C is very low (almost non-porous) with respect to MHT materials. These results could be related to the aging time (24 h) required in HT-C synthesis, during complete dissolution and reprecipitation of small particles probably take place, contributing mostly to the specific surface area and leading to the formation of larger crystals potentially blocking the pores, significantly influencing the textural properties of these materials [3,52]. The proposed combined mechanochemical/coprecipitation approach avoids the aging step, notably enhancing HT textural properties.

Pore size distribution for these materials, calculated according to the Barrett, Joyner, and Halenda (BJH) method (Figure 4), reveals significative modifications in the pore diameter values between HT synthesized by the conventional method and the hydrotalcites obtained by the combination of mechanochemistry/coprecipitation. The HT-C material presents a pore diameter range between 8 and 10 nm, indicating the presence of mesopores with a uniform structure. The materials synthesized by mechanochemistry/coprecipitation present pore size enlargement with a range of 5–45 nm for MHT-30 and MTH-60 materials and 3–40 nm for MHT-10, suggesting the presence of mesopores in the structure of these materials [53,54]. However, for the synthesized materials with longer grinding times (30 and 60 min), non-uniform mesopores are present due to the contribution of pores in the range between 1.5 and 4 nm, which can be attributed to mesopores with a very small structure (smaller mesopores and some micropores), possibly related to crystallite size [55]. In general, these results indicate that the combination of the mechanochemical/coprecipitation process promotes an increase in pore density due to the aggregation of the laminar-shaped layers with slit-shaped pores characteristic of hydrotalcites.

The SEM micrographs of the synthesized materials are shown in Figure 5. The materials prepared by the mechanochemical/coprecipitation combination method exhibit a notable propensity for agglomeration, displaying a spongy structure attributable to the overlapping of the typical sheets found in these materials. This agglomeration arises from a high surface/volume ratio, where the agglomerates are composed of numerous round particles possessing a

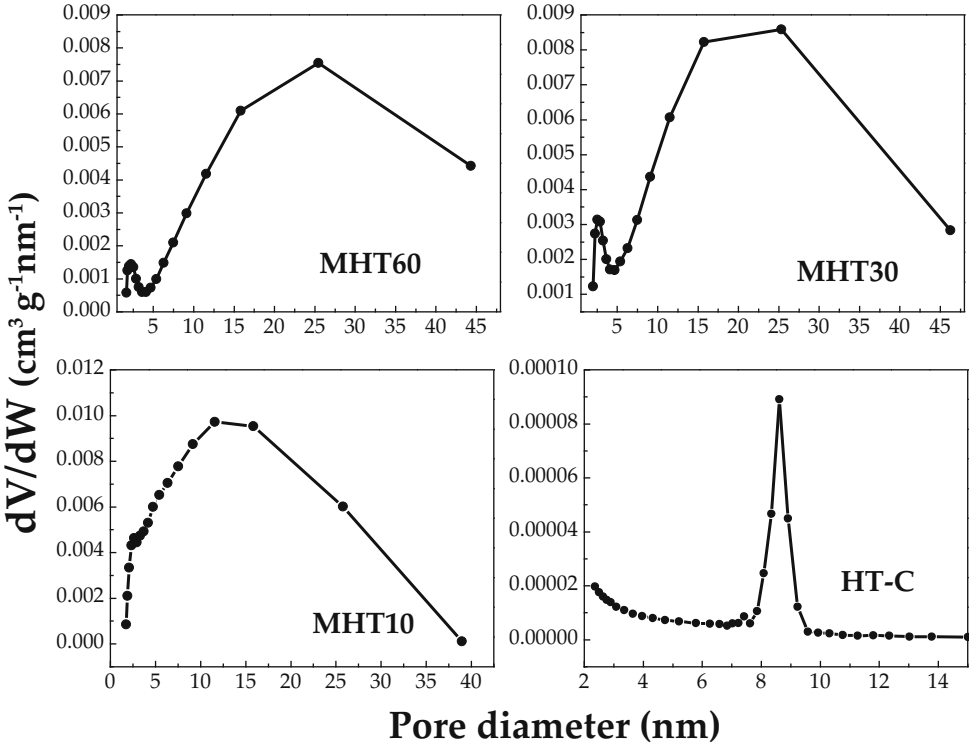

Figure 4: Pore size distribution of the hydrotalcites synthesized by the combined mechanochemical/coprecipitation method (MHT10, MHT30, MHT60) as compared to the conventional coprecipitation method HT-C.

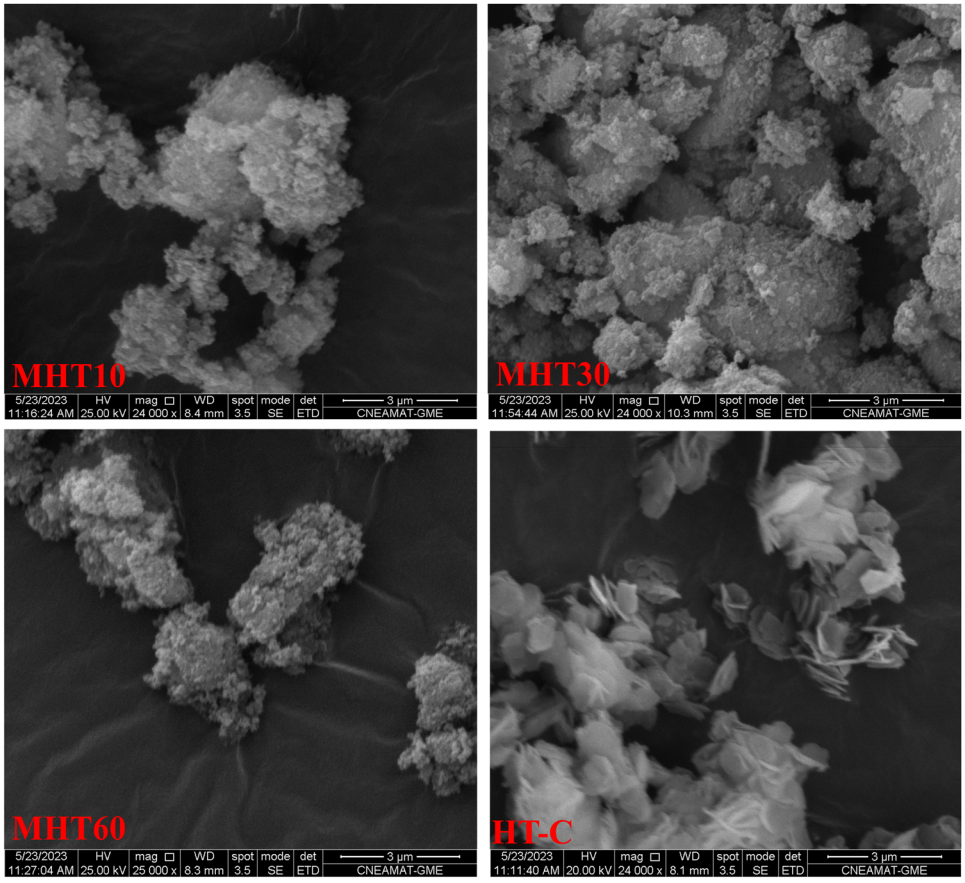

Figure 5: SEM images of hydrotalcites synthesized by the combined mechanochemical/coprecipitation method (MHT10, MHT30, MHT60) and the conventional coprecipitation method (HT-C).

very fine laminar structure characteristic of hydrotalcite materials [18]. In the mechanochemical process, when two adjacent particles collide, they share a common crystallographic orientation, leading to the amalgamation of two particles into a secondary one, thus promoting the spread of agglomeration and the formation of diminutive sheets [17]. In contrast, materials synthesized *via* the coprecipitation method (HT-C) show well-defined sheets with a larger laminar morphology. These results suggest that the combination of the coprecipitation/mechanochemistry method enhances the formation of smaller overlapping sheets, thereby generating compact agglomerates, corroborating the crystallite size and textural properties results. The morphology achieved by this method closely resembles that reported by other researchers utilizing coprecipitation, hydrothermal, and mechanochemical methods that necessitate extended synthesis durations (>5 h) [56–58].

The infrared spectrum for the synthesized materials shows characteristic bands typical of HT-type materials (Figure S1). Signals between 2,700 and 3,700 cm^{-1} correspond to stretching vibrations of the hydrogen bond in −OH groups and water molecules within the interlamellar region [36] (*e.g.*, band at 1,647 cm^{-1} is associated with deformation vibrations of water molecules present between layers) [26,59]. Interestingly, these bands display slight variations in the mechanochemical/coprecipitation materials, indicating a higher abundance of hydroxyl groups between the layers [60]. The band at 1,368 cm^{-1} is attributed to the antisymmetric stretching mode of the carbonate anion of the interlayer, while those at 667 and 871 cm^{-1} are related to vibrational modes of CO_3^{2-} species [61,62]. These bands suggest that carbonate ions are present as free anions, compensating for the positive charge of the laminar layers [63]. Notably, vibrational modes of the bicarbonate species are observed and designated to the region between 428 and 760 cm^{-1}, with small shoulders at 555 and 863 cm^{-1} [60]. The band around 452 cm^{-1} is attributed to the O–M bonds (M = metal) of the brucite layer, associated with the vibrational modes δHO-M-OH and δO-MO [64]. The characteristic signals of the vibrational modes of carbonate anions considerably decrease in mechanochemical/coprecipitated materials due to the observed increase in the parameter *c* in

these materials, linked to the formation of bicarbonate species in the interlaminar space, as described in XRD analysis.

To determine basic properties of the materials, CO_2 adsorption was conducted and analyzed using diffuse reflectance infrared Fourier transform spectroscopy (DRIFTS). CO_2 adsorption occurs by the formation of bidentate, monodentate, and bridged species arising from different types of basic surface sites [65]. Specifically, CO_2 adsorption on oxygen ions with the lowest coordination number leads to strong basic sites (monodentate species), whereas adsorption of bidentate carbonate species, bridged carbonates, and bicarbonate species leads to moderate and weak basic sites [23]. The signals at 1,680, 1,666, 1,640, 1,600, and 1,350 cm^{-1} correspond to ν_3 vibrational modes of the bidentate species, bridged carbonates, or bicarbonates (weak basic species), while signals between 1,308 and 1,248 cm^{-1} correspond to ν_3 vibrational modes of the monodentate species, associated to strong basic sites [65,66]. MHT materials exhibited a higher prevalence of basic sites (both strong and weak) compared to HT-C (Figure 6). Surprisingly, strong basic sites were observed to increase with longer grinding times, while weak basic sites decreased. This increase in strong and weak basic species in materials synthesized *via* the mechanochemical/coprecipitation approach could be attributed to the partial substitution of carbonate anions with the bicarbonate species due to a lower cationic charge in the layered structure, which is compensated for these species (consistent with the XDR results). Importantly, the proposed mechanochemical/coprecipitation approach allows for fine-tuning of the basic properties in HTs based on the milling time, which is critical for designing advanced catalytic (basic) materials in chemical reactions.

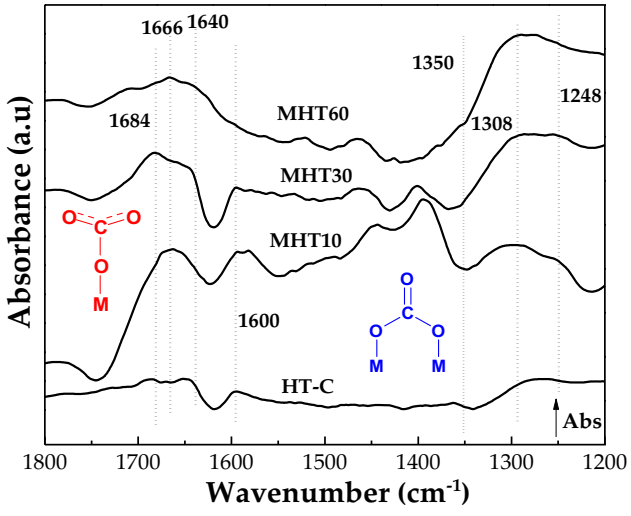

Figure 6: DRIFT-CO_2 analysis of hydrotalcites synthesized by combined mechanochemical and coprecipitation methods (MHT10, MHT30, and MHT60) or conventional coprecipitation method (HT-C). Monodentate species (blue) and bidentate species or bicarbonate (red).

The synthesized materials underwent testing in the Knoevenagel condensation reaction between furfural and ethyl cyanoacetate/malononitrile under solvent-free conditions. Initially, the reaction was conducted at 80°C for 30 min, with the results from Table S1 indicating high yields of the condensation product and high catalytic activity for all materials (>95% yields). Blank runs yielded low conversion (<10%) in the systems, confirming the necessity of a catalyst for the reaction. No significant differences were observed between HT-C and MHT materials under these preliminary investigated reaction conditions.

Subsequently, the reaction temperature was lowered to 40°C and room temperature (RT), revealing notable differences in terms of catalytic activity between HT-C and MHT materials (Figure 7). Compared to quantitative product yields (for ethyl cyanoacetate and malononitrile) obtained for MHT materials, HT-C exhibited a lower product yield of 35–50% under otherwise identical reaction conditions. These results clearly illustrate the observed enhancements in textural, morphological, and surface properties, as well as tunable basicity, exerting a critical influence on the catalytic activity of HT materials.

To gain a deeper understanding of the behavior of these materials, the reaction was studied using smaller amounts of the catalyst (Figure 8). As expected, a reduction in catalyst mass resulted in lower yields of the desired product. However, no significant differences were observed between the materials when the catalyst mass was decreased, maintaining an almost constant trend in yields toward the desired product. For instance, yields close to 30% were obtained with 10 mg of catalyst, while yields between 30 and 35% were achieved with 40 mg.

These findings suggest that the catalytic activity in the Knoevenagel condensation of furfural with ethyl cyanoacetate is not determined by the proportion of basic sites in the materials but rather by their basic character. CO_2-DRIFT analysis revealed the presence of both strong and weak basic species in all materials, with different proportions. For example, in the case of HT-C, weak basic sites (1.3 mmol/g titration with benzoic acid/bromothymol blue) predominated over strong basic sites (0.4 mmol/g titration with phenolphthalein). This suggests that the high presence of weak basic species in HT-C leads to lower yields, as Knoevenagel condensations are favored by strong basic sites. It is well known that extracting a proton from a methylene compound with a high pK_a value necessitates the presence of a catalyst with strong basic properties. Therefore, malononitrile and ethyl cyanoacetate, with pK_a values of 11.4 and 9, respectively, require strong basic sites

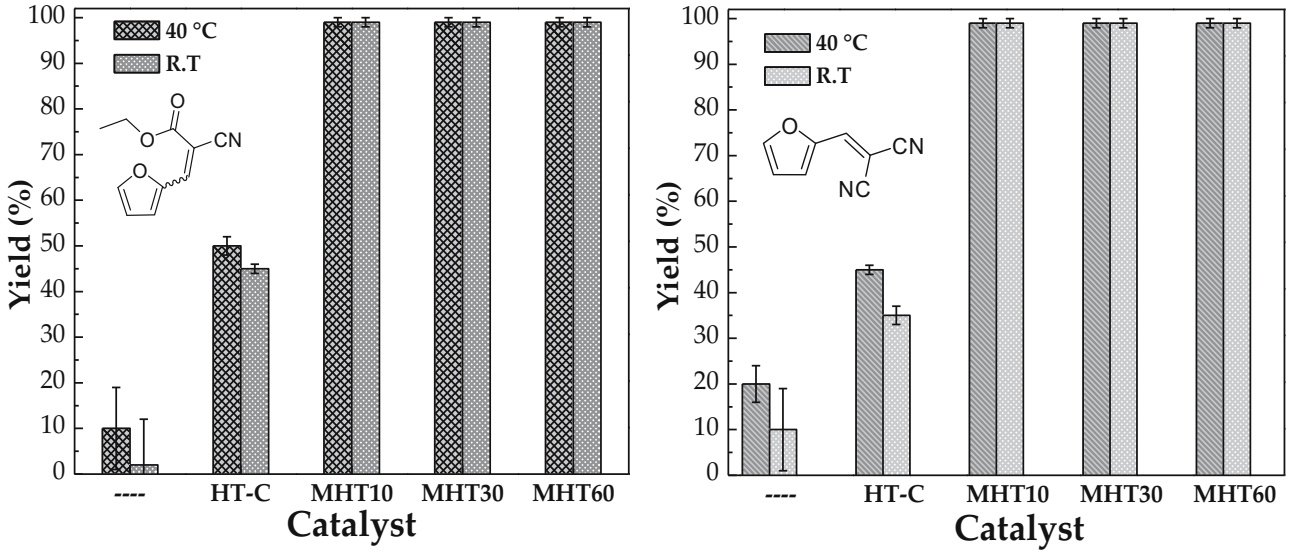

Figure 7: Knoevenagel condensation with hydrotalcites synthesized by mechanochemistry and the hydrotalcite synthesized by conventional coprecipitation. Reaction conditions: furfural (1 mmol), ethyl cyanoacetate/malononitrile (1 mmol), 80 mg catalyst, 10 min, and solvent-free.

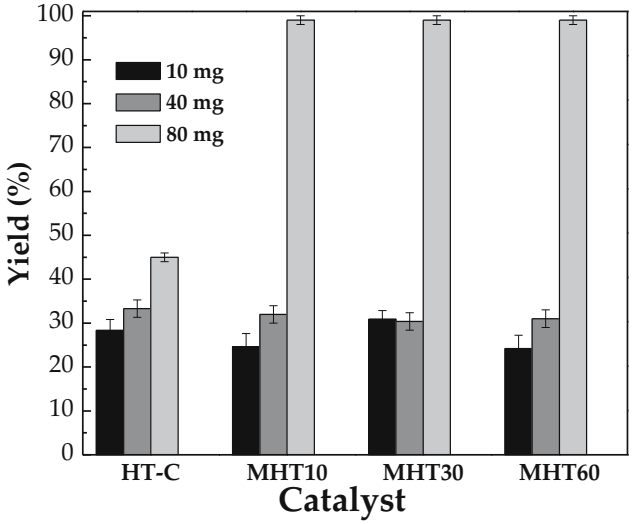

Figure 8: Mass of the catalyst in the Knoevenagel condensation. Reaction conditions: furfural (1 mmol), ethyl cyanoacetate (1 mmol), 10 min, solvent-free, and room temperature.

for their deprotonation and the formation of the corresponding carbanion [67]. The grinding process facilitates the generation of strong basic sites, which exhibit an escalating trend with extended grinding time (MHT10 = 0.723, MHT30 = 0.781, and MHT60 = 0.985 mmol/g), while concurrently reducing the presence of weak basic sites (MHT10 = 0.345, MHT30 = 0.140, and MHT60 = 0.187 mmol/g). However, there were variations in the abundance of strong basic sites between the different modified hydrotalcite (MHT), catalytic activity was affected by this parameter.

This behavior may be attributed to the crystallite size (2.7–3.5 nm), as no significant difference is observed among them. Moreover, the presence of small crystallites could promote higher surface activity in these materials due to increased pore density. However, a yield close to 45% is achieved for HT-C, which also has a small crystallite size (4.1 nm) under mild reaction conditions (room temperature and 10 min of reaction). These results indicate that the catalytic activity of these materials is not only influenced by their basic properties and crystallite size but may also be related to their morphological properties. It is noteworthy that HT-C exhibits a plate-like morphology, while MHT displays a granular morphology. This morphological variation significantly impacts the textural properties of the materials, as evidenced by an increase in the surface area for MHT. This increase facilitates greater availability of basic sites on the surface, thereby promoting the Knoevenagel condensation between furfural and malononitrile under mild reaction conditions. Consequently, the induced change in the morphology of these materials by the combination of mechanochemical/coprecipitation processes leads to a significant improvement in the catalytic activity of hydrotalcites in the Knoevenagel condensation reaction, in good agreement with previous investigations [68,69].

The presence of strong basic sites in modified hydrotalcite materials (MHT) and granular morphology provides a highly promising approach to obtaining high-value-added chemicals through the Knoevenagel condensation reaction of furfural. Various investigations have explored different reaction conditions, such as the use of solvents, acidic or

Table 2: Conditions and yield in the Knoevenagel condensation between furfural and malononitrile using other catalysts

Entry	Catalyst	Temperature (°C)	Time (min)	Yield (%)	Ref
1	SO_4^2/ZrO_2	Heated reflux	30	87	[74]
2	Co-MOF	40°C	30	100	[75]
		60°C	20	100	
3	Prol-MSN (mesoporous silica nanoparticles)	RT	30	76	[67]
4	SBA-15-Alanine	150°C	15	91	[76]
5	16Alanine-MCM-41	100°C	30	88	[77]
6	ILS ionic (liquid-functionalized SBA-15)	120°C	3	95	[78]
		Microwave			
7	HT commercial/dimethylformamide	100°C	15	99	[79]
8	Calcined hydrotalcite/dimethylformamide	RT	30	98	[80]
9	MHT	RT	10	99	This work

RT: room temperature.

basic materials as catalysts, and different reaction times and temperatures. In this context, catalysts such as Darco (commercial carbonaceous materials) for 6 h [70], sulfated polyborate for 60 min at 70°C in water: ethanol (1:1) [71], $ZrPO_4$ for 8 h at 100°C [72], BCN (dicyanamide/boric acid) for 15 min in methylbenzene at 80°C [73], and recently organocatalysts in ethanol for 30 min at room temperature [67], have been evaluated, showing promising results but with considerable reaction times and energy consumption.

Table 2 shows the results of solvent-free reaction conditions for the Knoevenagel condensation of furfural with malononitrile, a significant reduction in reaction times with high yields towards the Knoevenagel product. These results underscore the versatility of the Knoevenagel condensation reaction mediated by acidic or basic sites, wherein the presence of strong basic species in MHT materials facilitates obtaining high yields of the condensation product in reduced reaction times at room temperature.

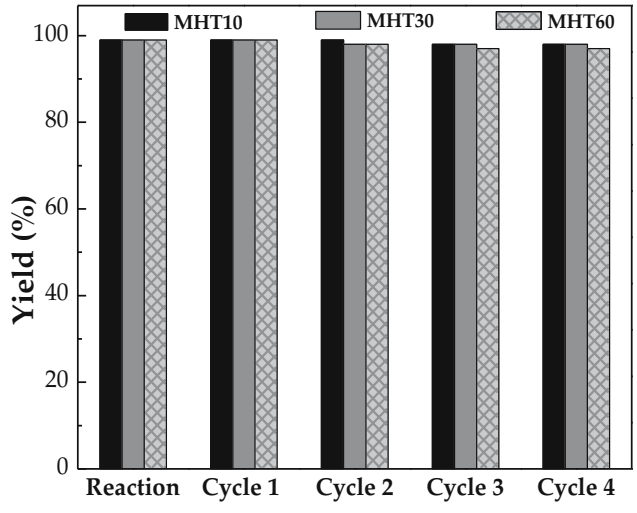

Figure 9: Reusability studies of MHT materials in four reaction cycles. Reaction conditions: furfural (1 mmol), ethyl cyanoacetate (1 mmol), 80 mg catalyst, 10 min, solvent-free (Reaction = starting reaction).

The results obtained in this work indicate a significant reduction in reaction times and high yields of the Knoevenagel product when utilizing MHT materials as catalysts in the absence of solvent within 10 min of reaction, representing a substantial improvement in terms of efficiency and energy consumption. Previous studies have demonstrated the efficiency of hydrotalcite-type materials (Table 2, entries 7 and 8). However, this work highlights the advantages of using hydrotalcite synthesized by a combination of mechanochemical process and coprecipitation method. This innovative approach opens new possibilities for designing more efficient and sustainable processes (less energy and time-consuming, solventless protocols) in the synthesis of materials and fine chemicals, thereby contributing to a more sustainable (nano)materials design.

In addition to the superior catalytic activities registered for MHT materials, reusability studies also confirmed the high stability and relevant unchanged activities preserved after 4 reaction cycles (Figure 9, Table S2) for all MHT materials.

4 Conclusions

The synthesis of hydrotalcite-type materials was revisited using a simple and efficient combined mechanochemical/coprecipitation approach that allowed the preparation of better crystalline, porous, and basicity-tuned HTs in short synthesis times (typically 10–30 min), avoiding aging steps and long synthesis times (ca. 48 h, conventional coprecipitation synthesis) that were proved to lead to the formation

of impurities. Textural, morphology, crystalline, and basic properties could be remarkably improved by the partial replacement of carbonate anions with bicarbonate species in the mechanochemical step. Importantly, layered structure formation was not influenced by the grinding time, with 10 min being sufficient to obtain well-defined and highly active HT materials. Importantly, basic properties (and species) in the layered structure could also be fine-tuned and controlled on the basis of grinding time in the mechanochemical step, developing weak and strong basic species at short milling times and strong basic sites at longer grinding times. The catalytic activity is highly influenced by the change in the morphology of the hydrotalcites, and novel MHT materials provided quantitative yields to Knoevenagel products under solventless conditions at room temperature (10 min reaction), without any loss of catalytic activity after four reaction cycles, as compared to moderate to low product yields (35–50%) obtained for HT-C counterparts. The proposed innovative combined approach has the potential to pave the way to the design of advanced LDH-related materials in large quantities (typically over 10 g material per batch, highly reproducible) for additional catalytic/adsorption-related applications that will be reported in due course.

Acknowledgments: MCIN and CSIC are acknowledged for providing synchrotron radiation facilities. This research has been supported by the Researcher Supporting Project Number (RSP2024R1), King Saud University, Riyadh, Saudi Arabia.

Funding information: The Spanish beamline (BM25, SpLine) in the ESRF (Grenoble, France) through the proposal ref. 25-02-1011. F. Ivars-Barcelo gratefully acknowledges MCIN for the “Ramón y Cajal” fund with ref. RYC2020-029470-I. This publication was supported by the RUDN University Strategic Academic Leadership Program (R. Luque).

Author contributions: All authors have accepted responsibility for the entire content of this manuscript and approved its submission.

Conflict of interest: The authors state no conflict of interest.

Data availability statement: The datasets generated and/or analysed during the current study are available from the corresponding author on reasonable request.

References

[1] Kannan S. Catalytic applications of hydrotalcite-like materials and their derived forms. Catal Surv Asia. 2006;10:117–37.

[2] Bernard E, Zucha WJ, Lothenbach B, Mäder U. Stability of hydrotalcite (Mg-Al layered double hydroxide) in presence of different anions. Cem Concr Res. 2022;152:106674.

[3] Li F, Duan X. Applications of layered double hydroxides. In: Duan X, Evans DG, editors. Layered double hydroxides. Berlin, Heidelberg: Springer Berlin Heidelberg; 2006. p. 193–223.

[4] Conterosito E, Gianotti V, Palin L, Boccaleri E, Viterbo D, Milanesio M. Facile preparation methods of hydrotalcite layered materials and their structural characterization by combined techniques. Inorg Chim Acta. 2018;470:36–50.

[5] Othman MR, Helwani Z, Martunus, Fernando WJN. Synthetic hydrotalcites from different routes and their application as catalysts and gas adsorbents: A review. Appl Organomet Chem. 2009;23:335–46.

[6] Baláž P, Dutková E. Fine milling in applied mechanochemistry. Miner Eng. 2009;22:681–94.

[7] Avila-Ortiz CG, Juaristi E. Novel methodologies for chemical Activation in organic synthesis under solvent-free reaction conditions. Molecules. 2020;25:3579.

[8] Chitrakar R, Tezuka S, Sonoda A, Sakane K, Ooi K, Hirotsu T. A solvent-free synthesis of Zn–Al layered double hydroxides. Chem Lett. 2007;36:446–7.

[9] Tongamp W, Zhang Q, Saito F. Preparation of meixnerite (Mg–Al–OH) type layered double hydroxide by a mechanochemical route. J Mater Sci. 2007;42:9210–5.

[10] Tongamp W, Zhang Q, Saito F. Mechanochemical route for synthesizing nitrate form of layered double hydroxide. Powder Technol. 2008;185:43–8.

[11] Salmones J, Zeifert B, Garduño MH, Contreras-Larios J, Acosta DR, Serrano AR, et al. Synthesis and characterization of hydrotalcites by mechanical milling and conventional method. Catal Today. 2008;133-135:886–90.

[12] Zhang X, Qi F, Li S, Wei S, Zhou J. A mechanochemical approach to get stunningly uniform particles of magnesium–aluminum-layered double hydroxides. Appl Surf Sci. 2012;259:245–51.

[13] Ferencz Z, Kukovecz Á, Kónya Z, Sipos P, Pálinkó I. Optimisation of the synthesis parameters of mechanochemically prepared CaAl-layered double hydroxide. Appl Clay Sci. 2015;112–113:94–9.

[14] Zhang F, Hou W. Mechano-hydrothermal preparation of Li-Al-OH layered double hydroxides. Solid State Sci. 2018;79:93–8.

[15] Madhusha C, Munaweera I, Karunaratne V, Kottegoda N. Facile mechanochemical approach to synthesizing edible food preservation coatings based on alginate/ascorbic acid-layered double hydroxide bio-nanohybrids. J Agric Food Chem. 2020;68:8962–75.

[16] Qu J, He X, Chen M, Hu H, Zhang Q, Liu X. Mechanochemical synthesis of Cu-Al and methyl orange intercalated Cu-Al layered double hydroxides. Mater Chem Phys. 2017;191:173–80.

[17] Fahami A, Beall GW. Structural and morphological characterization of Mg0.8Al0.2(OH)2Cl0.2 hydrotalcite produced by mechanochemistry method. J Solid State Chem. 2016;233:422–7.

[18] Fahami A, Al-Hazmi FS, Al-Ghamdi AA, Mahmoud WE, Beall GW. Structural characterization of chlorine intercalated Mg-Al layered double hydroxides: A comparative study between mechanochemistry and hydrothermal methods. J Alloy Comp. 2016;683:100–7.

[19] Jiang Y, Yang Z, Su Q, Chen L, Wu J, Meng J. Preparation of Magnesium-Aluminum Hydrotalcite by Mechanochemical Method and Its Application as Heat Stabilizer in poly(vinyl chloride). Materials. 2020;13:5223.

[20] Nope E, Sathicq ÁG, Martínez JJ, Rojas H, Romanelli G. Hydrotalcites as catalyst in suitable multicomponent synthesis of uracil derivatives. Catal Today. 2021;372:126–35.

[21] Zeng H-Y, Deng X, Wang Y-J, Liao K-B. Preparation of Mg-Al hydrotalcite by urea method and its catalytic activity for transesterification. AIChE J. 2009;55:1229–35.
[22] Nishimura S, Takagaki A, Ebitani K. Generation of functional platelets from canine induced pluripotent stem cells. Green Chem. 2013;15:2026–42.
[23] Rubio-Zuazo J, Ferrer P, López A, Gutiérrez-León A, da Silva I, Castro GR. The multipurpose X-ray diffraction end-station of the BM25B-SpLine synchrotron beamline at the ESRF. Nucl Instrum Methods Phys Res Sect A: Accel Spectrom Detect Assoc Equip. 2013;716:23–8.
[24] de la Calle C, Pons C-H, Roux J, Rives V. A crystal-chemical study of natural and synthetic anionic clays. Clays Clay Miner. 2003;51:121–32.
[25] Rives V. Characterisation of layered double hydroxides and their decomposition products. Mater Chem Phys. 2002;75:19–25.
[26] Zhou W, Tao Q, Pan J, Liu J, Qian J, He M, et al. Effect of basicity on the catalytic properties of Ni-containing hydrotalcites in the aerobic oxidation of alcohol. J Mol Catal A. 2016;425:255–65.
[27] Allmann R, Jepsen HP. Die Struktur des Hydrotalkits. N Jahrbuch Min Mh. 1969;1969:544–51.
[28] Knobloch D, Pertlik F, Zemann J. Crystal structure refinements of buetschliite and eitelite: a contribution to the stereochemistry of trigonal carbonate minerals. N Jahrbuch Min Mh. 1980;5:230–6.
[29] Hibino T, Ohya H. Synthesis of crystalline layered double hydroxides: Precipitation by using urea hydrolysis and subsequent hydrothermal reactions in aqueous solutions. Appl Clay Sci. 2009;45:123–32.
[30] Tichit D, Layrac G, Alvarez MG, Marcu I-C. Formation pathways of MII/MIII layered double hydroxides: A review. Appl Clay Sci. 2024;248:107234.
[31] Adachi-Pagano M, Forano C, Besse J-P. Synthesis of Al-rich hydrotalcite-like compounds by using the urea hydrolysis reaction—control of size and morphology. J Mater Chem. 2003;13:1988–93.
[32] Naghash A, Etsell TH, Lu B. Mechanisms involved in the formation and growth of Al–Cu–Ni hydrotalcite-like precipitates using the urea hydrolysis scheme. J Mater Chem. 2008;18:2562–8.
[33] Liu Q, Wang C, Qu W, Wang B, Tian Z, Ma H, et al. The application of Zr incorporated Zn-Al dehydrated hydrotalcites as solid base in transesterification. Catal Today. 2014;234:161–6.
[34] Panda HS, Srivastava R, Bahadur D. Stacking of lamellae in Mg/Al hydrotalcites: Effect of metal ion concentrations on morphology. Mater Res Bull. 2008;43:1448–55.
[35] Kuśtrowski P, Chmielarz L, Bożek E, Sawalha M, Roessner F. Acidity and basicity of hydrotalcite derived mixed Mg–Al oxides studied by test reaction of MBOH conversion and temperature programmed desorption of NH3 and CO2. Mater Res Bull. 2004;39:263–81.
[36] Korolova V, Zepeda FR, Lhotka M, Veselý M, Kikhtyanin O, Kubička D. Environmentally benign synthesis of hydrotalcite-like materials for enhanced efficiency of aldol condensation reactions. Appl Catal A: Gen. 2024;669:119506.
[37] Iyi N, Matsumoto T, Kaneko Y, Kitamura K. Deintercalation of carbonate ions from a hydrotalcite-like compound: enhanced decarbonation using acid−salt mixed solution. Chem Mater. 2004;16:2926–32.
[38] Olszówka JE, Karcz R, Bielańska E, Kryściak-Czerwenka J, Napruszewska BD, Sulikowski B, et al. New insight into the preferred valency of interlayer anions in hydrotalcite-like compounds: The effect of Mg/Al ratio. Appl Clay Sci. 2018;155:84–94.
[39] Coral N, Brasil H, Rodrigues E, da Costa CEF, Rumjanek V. Microwave-modified hydrotalcites for the transesterification of soybean oil. Sust Chem Pharm. 2019;114:9–53.
[40] Kovanda F, Koloušek D, Cílová Z, Hulínský V. Crystallization of synthetic hydrotalcite under hydrothermal conditions. Appl Clay Sci. 2005;28:101–9.
[41] Zadaviciute S, Baltakys K, Bankauskaite A. The effect of microwave and hydrothermal treatments on the properties of hydrotalcite: A comparative study. J Therm Anal Calori. 2017;127:189–96.
[42] Pavel OD, Stamate A-E, Zăvoianu R, Bucur IC, Bîrjega R, Angelescu E, et al. Mechano-chemical versus co-precipitation for the preparation of Y-modified LDHs for cyclohexene oxidation and Claisen-Schmidt condensations. Appl Catal A: Gen. 2020;605:117797.
[43] Seftel EM, Popovici E, Mertens M, Van Tendeloo G, Cool P, Vansant EF. The influence of the cationic ratio on the incorporation of Ti4+ in the brucite-like sheets of layered double hydroxides. Micropor Mesopor Mater. 2008;111:12–7.
[44] Zhang G, Hu L, Zhao R, Su R, Wang Q, Wang P. Microwave-assisted synthesis of ZnNiAl-layered double hydroxides with calcination treatment for enhanced PNP photo-degradation under visible-light irradiation. J Photochem Photobiol A. 2018;356:633–41.
[45] Chang Q, Zhu L, Luo Z, Lei M, Zhang S, Tang H. Sono-assisted preparation of magnetic magnesium-aluminum layered double hydroxides and their application for removing fluoride. Ultrason Sonochem. 2011;18:553–61.
[46] Houssaini J, Naciri Bennani M, Arhzaf S, Ziyat H, Alaqarbeh M. Effect of microwave method on jasminaldehyde synthesis using solvent-free over Mg–Al–NO3 hydrotalcite catalyst. Arab J Chem. 2023;16:105316.
[47] Dubnová L, Smoláková L, Kikhtyanin O, Kocík J, Kubička D, Zvolská M, et al. The role of ZnO in the catalytic behaviour of Zn-Al mixed oxides in aldol condensation of furfural with acetone. Catal Today. 2021;379:181–91.
[48] Benito P, Herrero M, Labajos FM, Rives V. Effect of post-synthesis microwave–hydrothermal treatment on the properties of layered double hydroxides and related materials. , Appl Clay Sci. 2010;48:218–27.
[49] Szabados M, Ádám AA, Kónya Z, Kukovecz Á, Carlson S, Sipos P, et al. Effects of ultrasonic irradiation on the synthesis, crystallization, thermal and dissolution behaviour of chloride-intercalated, coprecipitated CaFe-layered double hydroxide. Ultrason Sonochem. 2019;55:165–73.
[50] Navarro RM, Guil-Lopez R, Fierro JLG, Mota N, Jiménez S, Pizarro P, et al. Catalytic fast pyrolysis of biomass over Mg-Al mixed oxides derived from hydrotalcite-like precursors: Influence of Mg/Al ratio. J Anal Appl Pyrolysis. 2018;134:362–70.
[51] Malherbe F, Forano C, Besse JP. Use of organic media to modify the surface and porosity properties of hydrotalcite-like compounds. Microporous Mater. 1997;10(1–3):67–84.
[52] Trujillano R, González-García I, Morato A, Rives V. Controlling the Synthesis conditions for tuning the properties of hydrotalcite-like materials at the nano scale. ChemEngineering. 2018;2:31.
[53] Martins JA, Faria AC, Soria MA, Miguel CV, Rodrigues AE, Madeira LM. CO_2 methanation over hydrotalcite-derived nickel/ruthenium and supported ruthenium catalysts. Catalysts. 2019;9:1008.
[54] Iruretagoyena D, Fennell P, Pini R. Adsorption of CO2 and N2 on bimetallic Mg-Al hydrotalcites and Z-13X zeolites under high pressure and moderate temperatures. Chem Eng J Adv. 2023;13:100437.

[55] Nakamura GR, Aida T, Niiyama H. Textural properties of layered double hydroxides: effect of magnesium substitution by copper or iron. Microporous Mesoporous Mater. 2001;47:275–84.
[56] Sharma SK, Kushwaha PK, Srivastava VK, Bhatt SD, Jasra RV. Effect of hydrothermal conditions on structural and textural properties of synthetic hydrotalcites of varying Mg/Al ratio. Ind Eng Chem Res. 2007;46:4856–65.
[57] Shekoohi K, Hosseini FS, Haghighi AH, Sahrayian A. Synthesis of some Mg/Co-Al type nano hydrotalcites and characterization. MethodsX. 2017;4:86–94.
[58] Zhang X, Li S. Mechanochemical approach for synthesis of layered double hydroxides. Appl Surf Sci. 2013;274:158–63.
[59] Gomes JFP, Puna JFB, Gonçalves LM, Bordado JCM. Study on the use of MgAl hydrotalcites as solid heterogeneous catalysts for biodiesel production. Energy. 2011;36:6770–8.
[60] Huyen LTK, Dat NT, Thao NT. Synthesis and characteristics of Mg-Ni-Al-CO3hydrotalcites for styrene oxidation. Vietnam J Chem. 2018;56:203–7.
[61] Chagas LH, De Carvalho GSG, Do Carmo WR, San Gil RAS, Chiaro SSX, Leitão AA, et al. Clinical and pathological evaluation of fibrolamellar hepatocellular carcinoma: a single center study of 21 cases. Mater Res Bull. 2015;64:207–15.
[62] Shabanian M, Hajibeygi M, Raeisi A. FTIR characterization of layered double hydroxides and modified layered double hydroxides. In: Layered double hydroxide polymer nanocomposites. Woodhead publishing series in composites science and engineering; 2020. p. 77–101.
[63] Chang X, Zhang X, Chen N, Wang K, Kang L, Liu Z-H. Oxidizing synthesis of Ni2+–Mn3+ layered double hydroxide with good crystallinity. Mater Res Bull. 2011;46:1843–7.
[64] Costa DG, Rocha AB, Diniz R, Souza WF, Chiaro SSX, Leitão AA. Structural Model Proposition and Thermodynamic and Vibrational Analysis of Hydrotalcite-Like Compounds by DFT Calculations. J Phys Chem C. 2010;114:14133–40.
[65] Du H, Williams CT, Ebner AD, Ritter JA. In situ FTIR spectroscopic analysis of carbonate transformations during adsorption and desorption of CO2 in K-promoted HTlc. Chem Mater. 2010;22:3519–26.
[66] Ramesh S, Devred F, van den Biggelaar L, Debecker DP. Hydrotalcites promoted by NaAlO2 as strongly basic catalysts with record activity in glycerol carbonate synthesis. ChemCatChem. 2018;10:1398–405.
[67] Ortiz-Bustos J, Cruz P, Pérez Y, Hierro Id. Prolinate-based heterogeneous catalyst for Knoevenagel condensation reaction: Insights into mechanism reaction using solid-state electrochemical studies. Mol Catal. 2022;524:112328.
[68] Muráth S, Varga T, Kukovecz Á, Kónya Z, Sipos P, Pálinkó I, et al. Morphological aspects determine the catalytic activity of porous hydrocalumites: the role of the sacrificial templates. Mater Today Chem. 2022;23:100682.
[69] Karádi K, Nguyen T-T, Ádám AA, Baán K, Sápi A, Kukovecz Á, et al. Structure–activity relationships of LDH catalysts for the glucose-to-fructose isomerisation in ethanol. Green Chem. 2023;25:5741–55.
[70] Xu M, Richard F, Corbet M, Marion P, Clacens J-M. Upgrading of furfural by Knœvenagel condensation over functionalized carbonaceous basic catalysts. Catal Commun. 2019;130:105777.
[71] Ganwir P, Bandivadekar P, Chaturbhuj G. Sulfated polyborate as Bronsted acid catalyst for Knoevenagel condensation. Results Chem. 2022;4:100632.
[72] Kumar A, Srivastava R. Zirconium phosphate catalyzed transformations of biomass-derived furfural to renewable chemicals. ACS Sustain Chem Eng. 2020;8:9497–506.
[73] Li X, Lin B, Li H, Yu Q, Ge Y, Jin X, et al. Carbon doped hexagonal BN as a highly efficient metal-free base catalyst for Knoevenagel condensation reaction. Appl Catal B: Environ. 2018;239:254–9.
[74] Reddy BM, Patil MK, Rao KN, Reddy GK. An easy-to-use heterogeneous promoted zirconia catalyst for Knoevenagel condensation in liquid phase under solvent-free conditions. J Mol Catal A: Chem. 2006;258:302–7.
[75] Liu Z, Ning L, Wang K, Feng L, Gu W, Liu X. A new imidazole-functionalized 3D-cobalt metal-organic framework as a high efficiency heterogeneous catalyst for Knoevenagel condensation reaction of furfural. J Mol Struct. 2020;1221:128744.
[76] Appaturi JN, Pulingam T, Rajabathar JR, Khoerunnisa F, Ling TC, Tan SH, et al. Acid-base bifunctional SBA-15 as an active and selective catalyst for synthesis of ethyl α-cyanocinnamate *via* Knoevenagel condensation. Microporous Mesoporous Mater. 2021;320:111091.
[77] Appaturi JN, Selvaraj M, Abdul Hamid SB. Synthesis of 3-(2-furylmethylene)-2,4-pentanedione using DL-Alanine functionalized MCM-41 catalyst *via* Knoevenagel condensation reaction. Microporous Mesoporous Mater. 2018;260:260–9.
[78] Parvin MN, Jin H, Ansari MB, Oh S-M, Park S-E. Imidazolium chloride immobilized SBA-15 as a heterogenized organocatalyst for solvent free Knoevenagel condensation using microwave. Appl Catal A: Gen. 2012;413–414:205–12.
[79] Shirotori M, Nishimura S, Ebitani K. One-pot synthesis of furfural derivatives from pentoses using solid acid and base catalysts. Catal Sci Technol. 2014;4:971–8.
[80] Kantam ML, Ravindra A, Reddy CV, Sreedhar B, Choudary BM. Layered double hydroxides-supported diisopropylamide: synthesis, characterization and application in organic reactions. Adv Synth Catal. 2006;348:569–78.